A molecularly imprinted electrochemiluminescence sensor for ultrasensitive HIV-1 gene detection using EuS nanocrystals as luminophore

Bahareh Babamiri, Abdollah Salimi, Rahman Hallaj

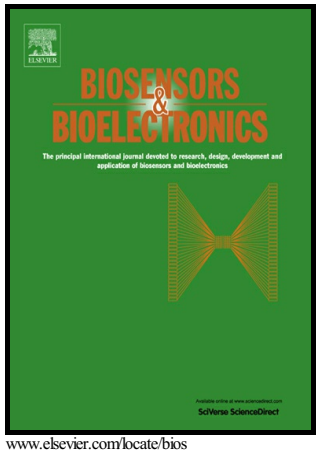

www.elsevier.com/locate/bios

PII: S0956-5663(18)30427-5
DOI: https://doi.org/10.1016/j.bios.2018.06.003
Reference: BIOS10523

To appear in: *Biosensors and Bioelectronic*

Received date: 20 March 2018
Revised date: 21 May 2018
Accepted date: 2 June 2018

Cite this article as: Bahareh Babamiri, Abdollah Salimi and Rahman Hallaj, A molecularly imprinted electrochemiluminescence sensor for ultrasensitive HIV-1 gene detection using EuS nanocrystals as luminophore, *Biosensors and Bioelectronic,* https://doi.org/10.1016/j.bios.2018.06.003

A molecularly imprinted electrochemiluminescence sensor for ultrasensitive HIV-1 gene detection using EuS nanocrystals as luminophore

Bahareh Babamiri, [a] Abdollah Salimi, [a,b*] Rahman Hallaj

[a]Department of Chemistry, University of Kurdistan, 66177-15175, Sanandaj, Iran

[b]Research Center for Nanotechnology, University of Kurdistan, 66177-15175, Sanandaj, Iran

Corresponding authors: Tel.: +98 8733624001; fax: +98 87336624008.

E-mail addresses: absalimi@uok.ac.ir, absalimi@yahoo.com (A. Salimi)

Abstract

Development of simple, sensitive and specific method for human immunodeficiency virus (HIV) assays are urgently demand. In this study, we developed a novel molecularly imprinted polymer (MIP) electrochemiluminescence (MIP-ECL) sensor for the highly sensitive and selective HIV-1 gene detection using Europium sulfide nanocrystals (EsNCs) as signal producing compound. Here, the HIV aptamer as the template and *o*-phenylenediamine as the functional monomer, were electropolymerized directly on the surface of ITO electrode. With the hybridization reaction between the assemblies of EuS NCs functionalized 5-amino-labeled oligonucleotides as capture probes and oligonucleotides as detection target (HIV gene), the ECL signal significantly increased using $K_2S_2O_8$ as coreactant. Taking advantage of both MIP-ECL assays and the strong electrochemiluminescence emission of EuS NCs, the sensitive and selective HIV gene detection has been achieved in a linear range 3.0 fM to 0.3 nM with a detection limit of 0.3 fM. The present MIP-ECL biosensor showed good specificity for HIV DNA detection compared to non-complementary and two bases mismatched sequences. The proposed ECL biosensor was applied to detect of HIV DNA in real human serum samples and satisfactory results were obtained. Due to high sensitivity and selectivity, excellent reproducibility and stability of the proposed assay, EuS NCs can be used as novel luminophore for development of MIP-ECL sensors for detection of other DNA biomarkers.

Keywords: Molecularly imprinted polymer, Electrochemiluminescence, HIV-1 gene sensor, EuS nanocrystal, Luminophore.

1. Introduction

Acquired immune deficiency syndrome (AIDS) is a severe communicable infectious disease caused by a retrovirus-the human immune deficiency virus (HIV), which destroys the body's natural protection from many diseases and usually leads to death (Ma, et al., 2017). The HIV/AIDS pandemic resulted in more than 39 million deaths worldwide since its discovery. Since, there are still no efficacious treatments, the early diagnosis and monitoring of HIV infection is a crucial aspect of controlling AIDS. There are two types of HIV viruses, known as HIV-1 and HIV-2, which HIV-1 is the most common cause of AIDS (Zhou, et al., 2015). Commonly, analysis of HIV antibody in serum was used to the diagnosis of HIV, but because of the existence of a "window period" in immunoassays which HIV antibody has not yet appeared in the sufferer's serum, an antibody test may give a 'false negative' result, even though a person is infected with HIV (Li, et al., 2014). So, nucleic acid detection can be efficacious approach for the early detection of HIV-1 infection without considering the window period in immunoassays. The hybridization between DNA or RNA probes and related complementary have been applied as usual assay for gene detection(Norrbakhash et al., 2011, Mansouri Majd et al., 2018a) .Up to now, blood tests including enzyme-linked immunosorbent assay (ELISA) (Karlsson, et al., 1991),enzyme immunoassay (EIA) (Janssen, et al., 1998), and Western blot test (Gong, et al., 2015), field effect transistors (FET) (Mansouri Majd et al., 2018 b) and electrochemical (Teymourian et al., 2017) are the most commonly used approaches for the HIV diagnosis in laboratories and hospitals. However, the above-mentioned techniques are often time-consuming, laborious, complicated and may require expensive instruments to operate, which leads to the limitation of these methods. Therefore, to

improve the survival rate and decrease therapy cost, the development of sensitive and specific analytical techniques for the detection of HIV at the earliest possible time are required for the identification of infected individuals and monitoring the disease progression. In recent years, molecularly imprinted polymers (MIPs) due to its superiorities such as desirable chemical and thermal stability, high adsorption capacity, effectively detection of specific molecules, excellent reusability, simplicity and low cost have been successfully applied for chemical/biological recognition (Xie, et al., 2010; Ning, et al ., 2014). Molecular imprinting technique (MIT) was first presented by Wulff in 1970s is a promising approach to identification specifically target (Wulff, et al., 1973). Actually, MIPs are also called plastic antibodies that synthesized by polymerizing of functional monomers and cross-linker around a template molecule (Cheong, et al., 2012; Volkert and Haes 2014). However, disadvantages such as low-affinity binding, incomplete template removal, low rate of mass transfer, lack of conductivity and electrocatalytical activity leads to the limitation of conventional MIPs (Alexander, et al., 2016). Hence, in order to overcome these shortcomings, the concept of molecular imprinting has been extended toward molecular imprinting polymers (MIPs) by imprinting of target molecules on the solid surface (Grinsven, et al., 2016). The template analytes in surface imprinting polymers approach can be biological molecule, cell and bacteria (Schirhagl, et al., 2012; Ren and Zare 2012; Dickert and Hayden 2002). On the other hand, the efficiency and sensitivity of the MIP sensors depends on the approaches of signal readout. So far, several electrochemical (Xie, et al., 2010), fluorescence (Yu, et al., 2017), and electrochemiluminescence (Wang, et al., 2016, Babamiri et al ., 2018d), sensors based molecularly imprinted polymer have been reported for detection of target

analyte. Among these methods, the electrochemiluminescent (ECL) techniques because of noteworthy advantages such as high sensitivity, low background signal, inexpensive instruments, excellent controllability and fast response is a promising analytical tool, which has also become a powerful analytical tool for the highly sensitive determination of the ultra-trace amounts of different targets in clinical diagnostics, environmental and biomolecule monitoring (Babamiri, et al ., 2018 a,b,c; Kong, et al., 2014; Yue, et al., 2016). This method intrinsically indicates a marriage between electrochemistry and spectroscopy that possesses the controllability and simplicity of electrochemistry with inherent sensitivity, low background and wide linear range of optical methods (Liu, et al ., 2015). Therefore, the MIP-ECL sensor, as a newly analytical device with the combination of the numerous superiorities of both MIP and ECL assays offered the advantages of high sensitivity, specificity and practicability, wide dynamic concentration response range, ease of miniaturization and automation at low cost, reusability and high precision and has been widely applied to detected different targets (Li, et al., 2013; Yang et al., 2016). During recent years, the continuously efforts have been done for the development of next-generation ECL emitting species (Zhao, et al., 2016; Fang, et al., 2011; Liu, et al., 2013). Nanomaterials based on rare-earth elements possess many advantages, such unique optical, electric, and magnetic properties that have attracted great attention in the field of applications in solar cells, fluorescent biolabeling and imaging (Wang, et al., 2013; Jiang, et al., 2010; Wang, et al., 2005; Zhao, et al., 2016; Zhao, et al., 2006). As a promising new luminescent material, EuS NCs because of their unique outstanding chemical, photo and magneto properties, narrow emission peak, long

fluorescence lifetime, high photochemical stability and low toxicity have attracted wide interest (Kataoka, et al., 2005; Zhao, et al., 2006)..

Herein, stable and water-soluble EuS nanocrystals (EuS NCs) capped with poly acrylic acid (PAA) as a novel electrochemiluminescent nanomaterials is prepared. Inspired by the excellent fluorescence property of EuS NCs, the cathodic ECL emission of EuS nanocrystals at the presence of $K_2S_2O_8$ as coreactant agent was investigated for the first time. Thus, a new methodology based on the ECL properties of EuS NCs and MIPs was explored for the diagnosis of HIV-1 infection that indicate the highly potential of EuS NCs for applications in the field of bioanalysis. In this present study, a novel sensitive and selective MIP-ECL sensor based on EuS nanocrystals (EuS NCs) for HIV DNA sequence determination has been developed. The EuS nanocrystals (EuS NCs) were used as luminescent signal source, and ultrathin imprinted film was formed by electropolymerization method using target (HIV DNA) as template and *o*-phenylenediamine as the functional monomer on the surface of ITO electrode. The experimental results illustrated that the proposed MIP-ECL sensor possesses many attractive characteristics such as, high sensitivity, high selectivity even against non-complementary and two-base mismatch sequences and good reproducibility which was successfully applied to the ultrasensitive determination of HIV DNA in human serum sample. The satisfactory results showed high performance of the presented strategy for detection of HIV DNA.

2. Experimental

2.1. Reagents and chemicals

The HIV related DNA strands utilized in the study were purchased from BIONEER, Global Genomics Partner and purified using HPLC. The detailed sequences of the oligonucleotides are summarized below:

5-end amino-modified ssDNA probe: 5-NH_2-GGGGGGCCAAGGCCCAGCCCTCACACA-3

HIV ssDNA target DNA sequence: 5-TGTGTGAGGGCTGGGCCTTGG-3

A two-base mismatched strand (mDNA): 5-TGTCTGAGGGCTCGGCCTTGG-3

Non-complementary strand (nDNA): 5-GGTTCCGGGTCGGGAGTGTGT-3.

The other chemicals and reagents is reported in SI.

2.2. Apparatus

The applied electrochemical, spectroscopic and imaging instruments are introduced in SI.

2.3. Synthesis and Surface Modification of EuS NCs

The details of procedure were used for synthesis of prepared nanocomposites reported in SI.

2.4. Preparation of the PAA-EuS NCs-DNA Probe

The 5′-amine modified of the HIV DNA strand was covalently bonded to the carboxyl group of the poly acrylic acid (PAA) stabilized EuS NCs as follow: Briefly, 0.4 mL of EDC (2 mg mL^{-1}) and 0.2 mL of NHS (2 mg mL^{-1}) were added to 5 mL of PBS (10 mM, pH 7.40) containing 5 mg of PAA-EuS NCs. The mixture was incubated at room temperature for 2 h with continuous stirring. Then, the activated PAA-EuS NCs were centrifuged and dispersed in 4.5 mL of PBS solution, after that 500 μL of HIV DNA capture probe was added to this mixture. The linkage reaction was processed at 37 °C another 2 h. Finally, the HIV DNA capture probe-conjugated PAA-EuS NCs were centrifuged, washed, and dispersed in in fresh PBS.

2.5. Fabrication of molecular imprinted polymer modified electrode

Both MIP and non-imprinted polymers (NIP) modified electrode were constructed by electropolymerization of the HIV ssDNA target sequence as template and *o*-phenylenediamine as the functional monomer on the surfaces of the electrodes. MIP electrodes were constructed using cyclic voltammetry from a solution containing 5 mM *o*-phenylenediamine and 20 µM template HIV aptamer in acetate buffer of pH 5.2, using a three-electrode assembly with the ITO as a working electrode, platinum as a counter electrode, and Ag/AgCl as a reference electrode for 30 cycles in the potential range from 0.2 V to 0.8 V at a scanning rate of 50 mV s^{-1}. The modified MIP electrode was washed with ultrapure water and immersed in ethanol water (10:2, v/v) solution containing 0.1 M NaOH for 1 h to remove the HIV aptamer template and to obtain the MIP modified electrode. The NIP modified electrode was prepared under the same conditions without adding of template (HIV aptamer).

2.6. ECL detection

For HIV-1 gene detection, MIP modified electrode was immersed into the standard solution containing different concentrations of HIV-1 gene for 20 min. The electrode was washed with water to remove the unbound HIV-1 gene. Then, the modified electrode was immersed into the PAA-EuS NCs-DNA probe solution and incubated for 30 min. Subsequently, excess PAA-EuS NCs-DNA probe was washed off with water. Then, the modified electrode was immersed in 0.1 M PBS (pH 7.4) containing 0.01 M $K_2S_2O_8$ as the coreactant agent and the potential scanned from 0.0 to -1.6 V with a scan rate of 100 mV s^{-1}. In the detection process, the voltage of the photomultiplier tube was set to 800 V. The ECL signals related to the HIV-1 gene concentrations were measured by placing a band-pass filter of 570 nm before the PMT window.

3. Results and discussion

3.1. Morphology and Structure Characterization of EuS NCs and water-soluble EuS NCs

The size distribution and morphology of the prepared of oleic acid europium sulfide nanocrystals (OA-EuS NCs) and PAA-EuS NCs were characterized by HRTEM. As shown in the TEM image (Fig. 1A), the prepared oleic acid-capped EuS were spherical and monodisperse, with a uniform size of approximately 8-10 nm. The TEM images reveal that after PAA-modification, because of the formation of a thin PAA layer on the surface of the bare EuS NCs, the average uniform diameters were about 16-20 nm (Fig. 1B). The FTIR spectroscopy was utilized to investigate the successful conjugation of PAA on the surface of the EuS NCs (Figure 1C). The synthetic OA-EuS NCs showed two strong absorption peaks at 1450 and 1562 cm^{-1}, which attributed to the asymmetric and symmetric vibrations of the carboxylate anions on the surface of the OA-EuS NCs. The absorption bands at 2959 and 2875 cm^{-1} correspond to the asymmetric and symmetric vibrations of CH_2, in the long alkyl chain of oleic acid. After the ligand exchange with PAA, a new strong bands at 1730 cm^{-1}, indicated an increase in the amount of -COOH groups on the particle surface. The obtained results confirmed that that the OA-EuS NCs were successfully converted into hydrophilic EuS NCs by ligand exchange of OA with PAA. To characterize the optical properties of EuS NCs, the UV-vis absorption and fluorescence emission spectra were recorded. The UV-vis spectrum revealed that the EuS NCs exhibit a considerable UV-vis absorption band centered at approximately 315 nm (Figure 1D). The synthesized EuS NCs solution was bright brown under visible light, but exhibits bright blue luminescence under UV lamp irradiation with a wavelength of 365 nm (the inset in Figure 1D). Also, Figure 1E demonstrated the fluorescence spectra of OA-EuS NCs and PAA-EuS NCs. It can be seen that, the same emission peaks at around 550 nm was obtained and no significant difference in fluorescence intensity existed between OA- EuS NCs and PAA-EuS NCs. The ECL spectrum of the EuS NCs revealed a maximum wavelength at 575 nm with a slight red-shift (550

to 575 nm) in a comparison with the fluorescence spectrum (Figure 1F). The crystal structure of the prepared EuS NCs was investigated by X-ray diffraction (XRD) analysis. According to the XRD of the EuS NCs (Figure 2A), sharp diffraction peaks at of 25.90°, 29.95° and 42.88° in 2θ, corresponds to (111), (200) and (220) faces of the typical face-centered cubic EuS crystal structure were observed that, demonstrating the successfully formation of the EuS NCs (Figure 2A). The obtained results showed the good agreement with the JCPDS file for bulk EuS (JCPDS, pdf file 26-1419). The EDS spectrum illustrated that the composition is constituted by Eu and S (Figure 2B).

3.2. Morphological and structural characterization of MIP and NIP

The surface morphology of the MIPs and NIPs film on the surface of ITO electrode were analyzed and characterized using scanning electron microscopy (SEM). SEM images of the MIPs revealed that the MIPs film was uniform (Fig. 2C). As shown in Figure 2 D micrographs of NIP electrode illustrated relatively sparsely and unevenly distribution. The obtained results indicated that the MIPs provides a large surface area for the adsorption of the HIV-1 gene at the surface of modified ITO electrode. Also, to evaluate the film thickness on the surface of electrode, SEM images were obtained. SEM images illustrated that the thickness of the polymer is within the range of 6-8 μm (Fig. S1).

3.3. Characterization of MIP and NIP

The electropolymerization method was applied to form homogeneous polymer film on the surface of ITO electrode. Fig. 3A showed CV curves recorded during the co-polymerization process of *o*-phenylenediamine and HIV-1 gene. In the first CV scan, an oxidation peak at +0.6 V demonstrated the electrooxidation of *o*-PD. The peak current decreased with continuous CV scans and almost disappeared after 30 cycles. Moreover, the peak current of the template HIV-1

gene-PoPD/ITO electrode decreased significantly with an increasing number of CV scans, indicating that both the template HIV-1 gene and accessible PoPD progressively deposited onto the ITO surface. The obtained results suggested that the moderately Poly-*o*PD was deposited together with template HIV-1 gene onto the electrode surface and also deposition of template HIV-1 gene-Poly-oPD increased with the number of scans.

3.4. EIS Monitoring of the biosensor construction

To investigate the changes of electrode behavior after each assembly step, CV was performed by using $[Fe(CN)_6]^{3-/4-}$ as the probe to illustrate the formation of the MIP film on the surface of electrode (Fig. 3B). As shown in Fig. 3A, obvious redox peaks can be found in the CV of bare ITO (curve a). After the electropolymerization of o-phenylenediamine and HIV-1 gene, redox peaks (curve b) disappeared, because the electron transfer between the surface of the electrode and the $[Fe(CN)_6]^{3-/4-}$ was influenced by the thickness of the MIP film. After the removal of HIV-1 gene, more imprinted cavities in the MIP film, more $[Fe(CN)_6]^{3-/4-}$ penetration channels for electrochemical redox and then the current would increase. The current decreased again, when the HIV-1 gene were captured by the MIP film.

Fig. 3C provided the impedance changes on the electrode during the binding, elution and rebinding processes. The bare ITO electrode showed the relatively low resistance. (curve a). When MIP film was formed on the surface of ITO electrode, the resistance obviously increased (R_{ct}=6300 Ω, curve b). In the following, with elution the HIV ssDNA target DNA sequence, from the imprinted polymer, cavities act as the channels for electron transfer and decreasing in resistance was observed (R_{ct}=1450 Ω, curve c). Subsequently, when the HIV ssDNA target DNA sequence was captured, the resistance of MIP-based electrode increased again because the channels of electron transfer would be blocked and the electron transfer rate decreased (R_{ct}=2750

Ω, curve d). Finally, with the successive formation of the EuS NCs-ssDNA probe/ HIV ssDNA target DNA sequence duplex on the MIP, the resistance increased (R_{ct}=3450 Ω, curve e). These changes in the electron transfer resistance confirmed that the ECL biosensor was successfully fabricated.

Also, according to the XRD of the modified electrode (Fig. S2), sharp diffraction peaks at of 25.90°, 29.95° and 42.88° in 2θ, corresponds to (111), (200) and (220) faces of the typical face-centered cubic EuS crystal structure were observed, which demonstrate the successfully immobilization of the EuS NCs on the surface of electrode through the hybridization of HIV ssDNA target DNA sequence and ssDNA-EuS NCs probe.

3.5. Characterization of the PAA-EuS NCs-ssDNA probe conjugate

To investigate the successful immobilization of ssDNA probe onto the PAA-EuS NCs, the optical absorption spectra of PAA-EuS NCs and PAA-EuS NCs-ssDNA probe were recorded. An obvious change in the intensity of absorption was observed, that indicating the successful immobilization of ssDNA probe onto the PAA-EuS NCs (Fig. S3). The obtained result indicated that the ssDNA had been completely conjugated with the PAA-EuS NCs.

3.6. Investigation of the sensing mechanism of HIV-1 gene and ECL response of the EuS NCs

When the imprinted polymer incubated by the ssDNA target DNA sequence, the EuS NCs-ssDNA probe can be introduced to the electrode through the successive formation of the EuS NCs-ssDNA probe/HIV ssDNA target DNA sequence duplex. Finally, the bioconjugation of MIP-HIV ssDNA target DNA sequence /ssDNA -EuS NCs can generate intensive ECL emission in pH 7.40 PBS with 0.01 M $K_2S_2O_8$ as the coreactant. While, in the absence of the HIV ssDNA target DNA sequence, the EuS NCs-ssDNA probe cannot effectively introduced to the surface of electrode. So, the negligible ECL signal was observed (Fig. S4).

The cathodic ECL behavior of EuS NCs at ITO electrode were studied. In the presence of co-reactant $S_2O_8^{2-}$ ions by generation of $SO_4^{\bullet-}$ radicals, the immobilized EuS NCs on the electrode were reduced to be $(EuS)^{\bullet-}$ NCs by charge injection. With the reaction between the $(EuS)^{\bullet-}$ and $SO_4^{\bullet-}$, a strong ECL emission peak at -1.45 V with an onset potential of -0.8 V was obtained. The probable ECL mechanisms could be stated with the following equations (Guo, et al., 2016) (1) - (4):

$$EuS\ NCs + e^- \rightarrow (EuS\ NCs)^{\bullet-} \quad (1)$$

$$S_2O_8^{2-} + e^- \rightarrow SO_4^{2-} + SO_4^{\bullet-} \quad (2)$$

$$(EuS\ NCs)^{\bullet-} + SO_4^{\bullet-} \rightarrow EuS\ NCs^* + SO_4^{2-} \quad (3)$$

$$EuS\ NCs^* \rightarrow EuS\ NCs + h\nu \quad (4)$$

3.7. The determination of HIV DNA

Under the optimized experimental conditions, the quantitative measurements of the HIV ssDNA target DNA sequence was carried out with the prepared MIP-ECL sensor. With the increasing concentration of HIV ssDNA target DNA sequence bound into the imprinted cavities, more EuS NCs-ssDNA probe can be introduced to the surface of electrode. According to Figure 4A, the ECL intensity increased gradually with the increasing concentration of the target HIV-1 gene from 3 fM to 0.3 nM. As displayed in Figure 4B, the linear regression equation I (a.u.) = 152.02 lg C- 19.605 with a correlation coefficient of 0.99 was obtained (where I stands for the ECL intensity and c stands for HIV DNA concentration). The detection limit (LOD) was evaluated to be 0.3 fM at a signal-to-noise ratio of 3. In a comparison with previously reported methods for HIV-1 gene detection, the MIP-ECL sensor based on the EuS NCs/$K_2S_2O_8$ ECL system showed a higher sensitivity and lower limit of detection (Table 1A). Compared to the other luminophore

system for ECL detection (Table S1), the novel EuS NCs/$K_2S_2O_8$ ECL system showed the high analytical performance.

3.8. Specificity, reproducibility and stability of the MIP sensor

To investigate the recognition specificity of the MIP sensor toward to HIV ssDNA target DNA sequence, the ECL signal using EuS NCs-ssDNA to hybridize with three kinds of DNA sequences, including HIV ssDNA target DNA sequence, two-base mismatched DNA and non-complementary DNA at the same concentration were recorded. As illustrated in Figure 4C, it can be seen that there was no obvious ECL signal at the presence of two-base mismatched DNA as target and there was approximately no change in the ECL responses of non-complementary DNA compared with HIV ssDNA target DNA sequence because the non-complementary DNA could not be hybridized with the EuS NCs-ssDNA probe. Obviously, these results demonstrated that the prepared MIP has excellent specificity for HIV ssDNA target DNA sequence. Furthermore, the non MIP-ECL sensor showed very little the ECL responses compared with the MIP-ECL sensor (Figure 4C). The obtained results suggested that the non MIP could not effectively bind HIV ssDNA target DNA sequence. The reproducibility of the proposed biosensor was evaluated by measuring the ECL signal of 0.1 nM HIV DNA using five different sensors under the same condition. The relative standard deviations (RSD) of the five independent assays was 5.11 %, indicating a desirable accuracy and reproducibility of the ECL assay (Figure S7). To investigate the storage stability of the presented biosensor for the determination of HIV DNA, ECL intensity after 3 weeks of storage in 4 °C were recorded. The obtained results indicated that the MIP-ECL sensor retains about 95% of its original response for 0.1 nM HIV DNA. So, the proposed HIV DNA biosensor has acceptable storage stability, it can be used for a sufficiently long time. The ECL intensities of the MIP-ECL sensor was recorded under continuous potential scanning for 12

cycles. The relative standard deviation (RSD) was less than 2.16 %, indicating an acceptable stability of the proposed sensor for ECL detection (Figure 4D).

3.9. Analysis of HIV-1 gene in serum samples

For assessing the feasibility and potential applicability of the proposed assay, the recovery experiments in real sample was employed to determine HIV DNA target in serum samples. The human serum samples were obtained from the Verdi Clinical laboratory in Sanandaj of Iran. The serum samples were spiked with different concentrations of HIV DNA target and detected by the proposed sensor. As shown in Table 1B, the recoveries and RSD were in the range of 95.00−101.2% and of 1.78 to 4.2%. The satisfactory results indicated that the ECL sensor synthesized by surface imprinting procedure exhibited good sensitivity and a high percentage recovery in biological sample.

4. Conclusions

In summary, a novel MIP-ECL sensor based on the ECL signal of EuS NCs for the sensitive detection of HIV-1 gene has been developed. Herein, the established MIP film on the surface of ITO electrode via a typical electropolymerization method can specifically capture and selectively recognize the HIV ssDNA target DNA sequence. EuS nanocrystals (EuS NCs) possess many advantages, such as narrow emission peak, long fluorescence lifetime, high photochemical stability and low toxicity. The proposed sensor with the combination of the ECL behavior of EuS NCs and excellent specificity of molecular imprinting technique successfully applied for the sensitive and selective detection of HIV-1 gene with the detection limit down to 0.3 fM. The obtained results demonstrated that the proposed MIP-ECL assay have outstanding features such as high sensitivity and selectivity, wide dynamic range, high precision. Also, the sensor can be a

promising candidate for analysis of other DNA sequences. The proposed method has the great potential for clinical applications in the analysis of HIV and other DNA sequences.

Acknowledgments

This research was supported by the Iranian Nanotechnology Initiative (109373) and the Research Office of the University of Kurdistan (4.1404086).

References

Alexander, S., Baraneedharan, P., Balasubrahmanyan, S., Ramaprabhu, S., 2016. Eur. Polym. J. 86, 106-116.

Babamiri, B., Hallaj, R., Salimi, A., 2018a. Sens. Actuator B 254, 551-556.

Babamiri, B., Hallaj, R., Salimi, A., 2018b. Biosens. Bioelectron. 102, 328-335.

Babamiri, B., Hallaj, R., Salimi, A., 2018c. Biosens. Bioelectron. 99, 353-360.

Babamiri, B., Salimi, A., Hallaj, R., Hasan zadeh, M., 2018d. Biosens. Bioelectron 107, 272-279.

Cheong, W., Yang, S., Ali, F., 2012. J. Sep. Sci. 36, 609-628.

Dickert, F., Hayden, O., 2002. *Anal. Chem.* 74, 1302-1306.

Fang, Y., Song, J., Li, J., Wang, Y., Yang, H., Sun, J., Chen, G., 2011. Chem. Commun. 47, 2369-2371.

Gong, Q., Wang, Y., Yang. H., 2017. Biosens. Bioelectron. 89, 565-569.

Gong, Q., Yang, H., Dong, Y., Zhang, W., 2015. Anal. Methods**. 7**, 2554-2562.

Grinsven, B., Eersels, K., Akkermans, O., Ellermann, S., Kordek, A., Peeters, M., Deschaume, O., Bartic, C., Diliën, H., Redeker, E., Wagner, P., Cleij, T., 2016. *ACS Sens.* 1, 1140–1147.

Guo, X., Wu, S., Duan, N., Wang, Z., 2016. Anal. Bioanal. Chem. 408, 3823-3831.

Yue, H., Zhou, Y., Wang, Wang, X., Wang, Zh., Wang, L., Fu, Zh., 2016. Biosens. Bioelectron. 153. 401-406.

Janssen, R., Satten, G., Stramer, S. L., 1998. JAMA. 280, 42-48.

Jiang, Y., Yang, X., Ma, C., Wang, C., Li, H., Dong, F., 2010. Small 6, 2673-2677.

Karlsson, R., Michaelsson, A., Mattsson, L., 1991. J. Immunol. Methods. 145, 229-240.

Kataoka, T., Tsukahara, Y., Wada, Y.,2005. Chem. Commun. 48, 6038-6040.

Li, B., Li, Z., Situ, B., Dai, Z., Liu, Q. Wang, Q., Gu, D., Zheng, L., 2014. Biosens. Bioelectron. 52, 330-336.

Li, H., Xie, C., Fu, X., 2013. Sens. Actuators, B 181, 858-866.

Liu, L., Ma, Q., Li, Y., Liu, Z. Su. X., 2015. Biosens. Bioelectron. 63, 519-524.

Liu, T., Zhang, L., Song, H., Lv, Y., 2013. Luminescemce 28, 530-535.

Ma,Y., Shen, X., Zeng, Q., Wang, H., 2017. Talanta 164, 121-127.

Mansouri Majd, S., Salimi, A., Ghasemi, F., 2018 a Biosens. Bioelectron.105, 6-13.

Mansouri Majd, S., Salimi, A., Astinchap B., 2018 b, Sens. Actuators B 266,178-186.

Ning, F., Peng, H., Chen, L., Xiong, H., Li, J., 2014. J. Agric. Food. Chem. 62, 7436-7443.

Noorbakhash, A., Salimi, A., 2011 Biosens. Bioelectron. 30,188-196.

Qaddarea, S. H., Salimi, A., 2017. Biosens. Bioelectron. 89, 773-780.

Ren, K., Zare, R., 2012. ACS Nano. 6, 4314-4318.

Schirhagl, R., Hall, E., Fuereder, I., Zare, R., 2012. Analyst 137, 1495-1499.

Teymourian, H., Salimi, A., Khezrian, S., 2017. Electroanalysis 29, 409-414.

Volkert, A., Haes, A., 2014. Analyst 139, 21-31.

Wang, K., Fan, D., Liu, Y., Dong. S., 2017. Biosens. Bioelectron. 87, 116-121.

Wang, L., Yan, R., Huo, Z., Wang, L., 2005. Angew. Chem. Int. Ed. 44, 6054-6057.

Wang, Q., Chen, M., Zhang, H., Wen, W., Zhang, X., Wang, S., 2016. Sens. Actuators, B 222, 264-269.

Wang, Y., Liu, G., Sun, L., Xiao, J., Zhou, J., Yan, C., 2013. *ACS Nano*. 7, 7200-7206.

Kong, W., Zhou, H., Ouyang, H., Li, Z., Fu, Zh., 2014. Anal. Methods 6, 2959-2964.

Wulff, G., Sarhan, A., Zabrocki, K., 1973. Tetrahedron Lett. 14, 4329-4332.

Xie, C., Gao, S., Guo, Q., Xu, K., 2010. Microchim. Acta 198, 145-152.

Xie, C., Li, H., Li, S., Wu, J., Zhang, Z., 2010. Anal. Chem. 82, 241-249.

Yang, B., Li, J., Zhang, L., Xu, G., 2016. Analyst 141, 5822-5828.

Yu, J., Wang, X., Kang, Q., Li, J., Shen, D., Chen, L., 2017. Environ. Sci. Nano**.** 4**,** 493-502.

Ye, Y., Xia, L., Xu, D., Xing, X., Pang, D., Tang, H., 2016. Biosens. Bioelectron. 85, 837-843.

Zhang, D., Peng, Y., Qi, H., Gao, Q., Zhang, C., 2010, Biosens. Bioelectron. 25, 1088-1094.

Zhao, M., Chen, A., Huang, D., Zhuo, Y., Chai, Y., Yuan, R., 2016. Anal. Chem. 88, 11527-11532.

Zhao, F., Sun, H, Su, G., Gao, S., 2006. Small 2, 244-248.

Zhao, F., Yuan, M., Zhang, W., Gao, S., 2006. J. Am. Chem. Soc. 128, 11758-11759.

Zhao, Y., Shi, C., Yang, X., Shen, B., Sun, Y., Chen, Y., Xu, X., Sun, H., Yu. K., Yang, B., Lin, Q., 2016. *ACS Nano* 10, 5856-5863.

Zhou, L., Huang, J., Yu, B., Liu, Y. You, T., 2015. ACS Appl. Mater. Interfaces. 7, 24438–24445.

Figures Captions

Scheme 1. Schematic representation of the MIP-ECL assay for the detection of HIV-1 gene.

Table 1A. Comparison the analytical performance of different methods for HIV-1 gene detection

Table 1B. A recovery study carried out in serum samples for HIV-1 gene determination by the proposed sensor

Fig. 1. (A) TEM image and Gauss fitting of particle size distribution of OA-EuS NCs (B) TEM image and Gauss fitting of particle size distribution of PAA-EuS NCs (C) FTIR spectra of OA-EuS NCs (a, red line) and PAA-EuS NCs (b, blue line), (D) UV−vis absorption of EuS NCs (The inset in part A:

photographs of the EuS NCs aqueous solution taken under visible light (lamp off) and 365 nm UV light (lamp on)), (E) PL spectra of OA-EuS NCs and PAA-EuS NCs, (F) ECL emission spectra of EuS NCs

Fig. 2. (A) XRD pattern of EuS NCs, (B) EDS spectra of EuS NCs, (C) SEM images of MIP electrode, (D) SEM images of NIP electrode,

Fig.3. (A) Cyclic voltammograms of the template HIV aptamer/PoPD/ITO in the acetate buffer of pH 5.2 at 50 mV s^{-1} scan rate vs. Ag/AgCl and 30 number of scans (B) CV curves of different modified electrode: (a) bare ITO; (b) PoPD MIP coated electrode; (c) PoPD MIP modified electrode after the removal of HIV aptamer and (d) HIV aptamer/PoPD/ITO modified electrode in a 10 mM PBS of pH 7.4 containing 1 mM $[Fe(CN)_6]^{3-/4-}$ and 0.1 mM KCl at 50 mV s^{-1} scan rate vs. Ag/AgCl, (C) Nyquist curves recorded in a solution of 0.1 M KCl containing 1 mM $[Fe(CN)_6]^{3-/4-}$at different electrodes (a) bare ITO (Inset carve), (b) MIP-ITO, (c) MIP-ITO after template removal, (d) MIP-ITO after rebinding of HIV aptamer, (e) MIP-ITO after hybridization of the HIV ssDNA target DNA sequence and ss capture probe DNA- EuS NCs, applied potential was 0.2 V at the frequency range of 0.1Hz-10kHz, Inset: the equivalent circuit applied to fit the impedance data. R_s, solution resistance; CPE, constant phase angle element; R_{ct}, electron-transfer resistance; W_o, Warburg diffusion resistance.

Fig.4. (A) ECL responses of the proposed sensor in different concentrations of HIV-1 gene in 0.1 M pH 7.4 PBS containing 10 mM $K_2S_2O_8$, scanning from 0 V to -1.6 V with a scan rate of 100 mV s^{-1}, (B) The corresponding relationship between the ECL intensity and the logarithm of HIV-1 gene concentration (RSD% from 3 fM to 0.3 nM, 4.2, 3.85, 5.61, 5.31, 4.91, 3.81, 4.95, 4.15 and 5.26), (C) Effects of target DNA, two-base mismatched strand, and non-complementary strand on the ECL signal response measured by the optimal MIP-ECL sensor and the ECL signal response measured by the optimal ECL sensor for MIP and NIP (D) The stability of the MIP-ECL developed sensor based EuS NCs/$K_2S_2O_8$ system under 12 consecutive cyclic potential scans.

Table 1A. Comparison the analytical performance of different methods for HIV-1 gene detection

Detection method	Linear range (M)	Detection limit (M)	Reference
Impedimetric	1.0×10^{-13}-1.0×10^{-10}	2.3×10^{-14}	(Gong, et al., 2017)
Electrochemical	10×10^{-18}-1.0×10^{-9}	2.0×10^{-18}	(Zhang, et al., 2010)
Electrochemical	40×10^{-9}-2.56×10^{-6}	5×10^{-9}	(Li, et al., 2014)
Colorimetric Assay	0.5×10^{-12}-1.0×10^{-9}	0.5×10^{-12}	(Wang, et al., 2017)
Fluorescence	1×10^{-9}-50×10^{-9}	0.4×10^{-9}	(Ye, et al., 2016)
Electrochemical	1.0×10^{-17}- 1.0×10^{-9}	2.0×10^{-18}	(Teymourian et al., 2017)
Field effect Transistor	1.0×10^{-18}- 1.0×10^{-8}	0.3 aM	Mansouri majd et al.,2018b)
Fluorescence	50×10^{-15}-1×10^{-9}	15×10^{-15}	(Qaddarea, et al., 2017)
MIP-Electrochemiluminesence	3×10^{-15}-0.3×10^{-9}	0.3×10^{-15}	This work

Table 1B. A recovery study carried out in serum samples for HIV-1 gene determination by the proposed sensor

Sample	Added (pM)	Found (pM)	Recovery (%)	RSD (%)
1	0.01	0.0095	95	1.78
	1	1.015	101.5	2.31
	10	10.21	102.1	3.2
	0.01	0.0101	101	4.12

2	1	0.985	98.5	3.5
	10	10.05	100.5	4.2

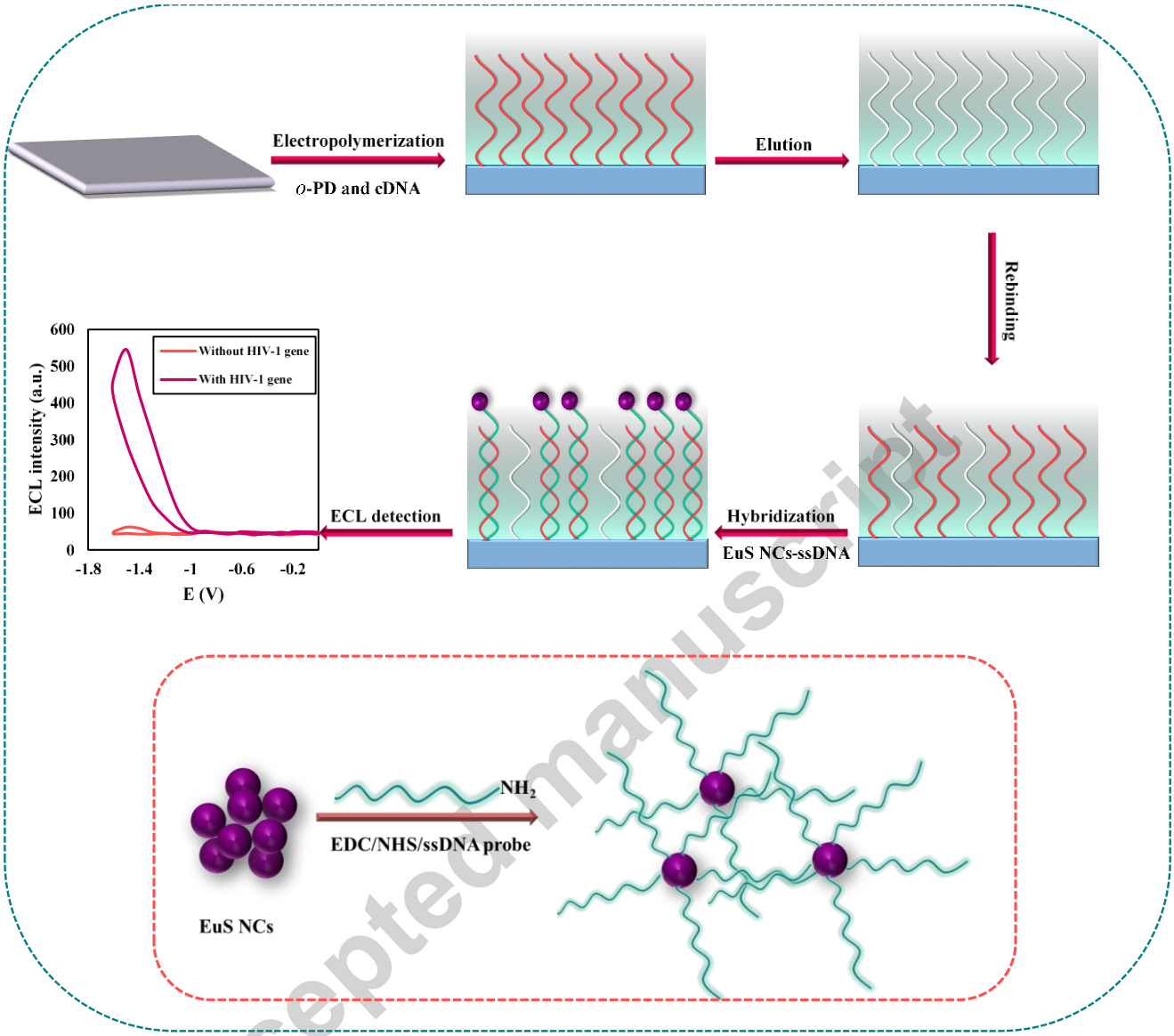

Scheme 1

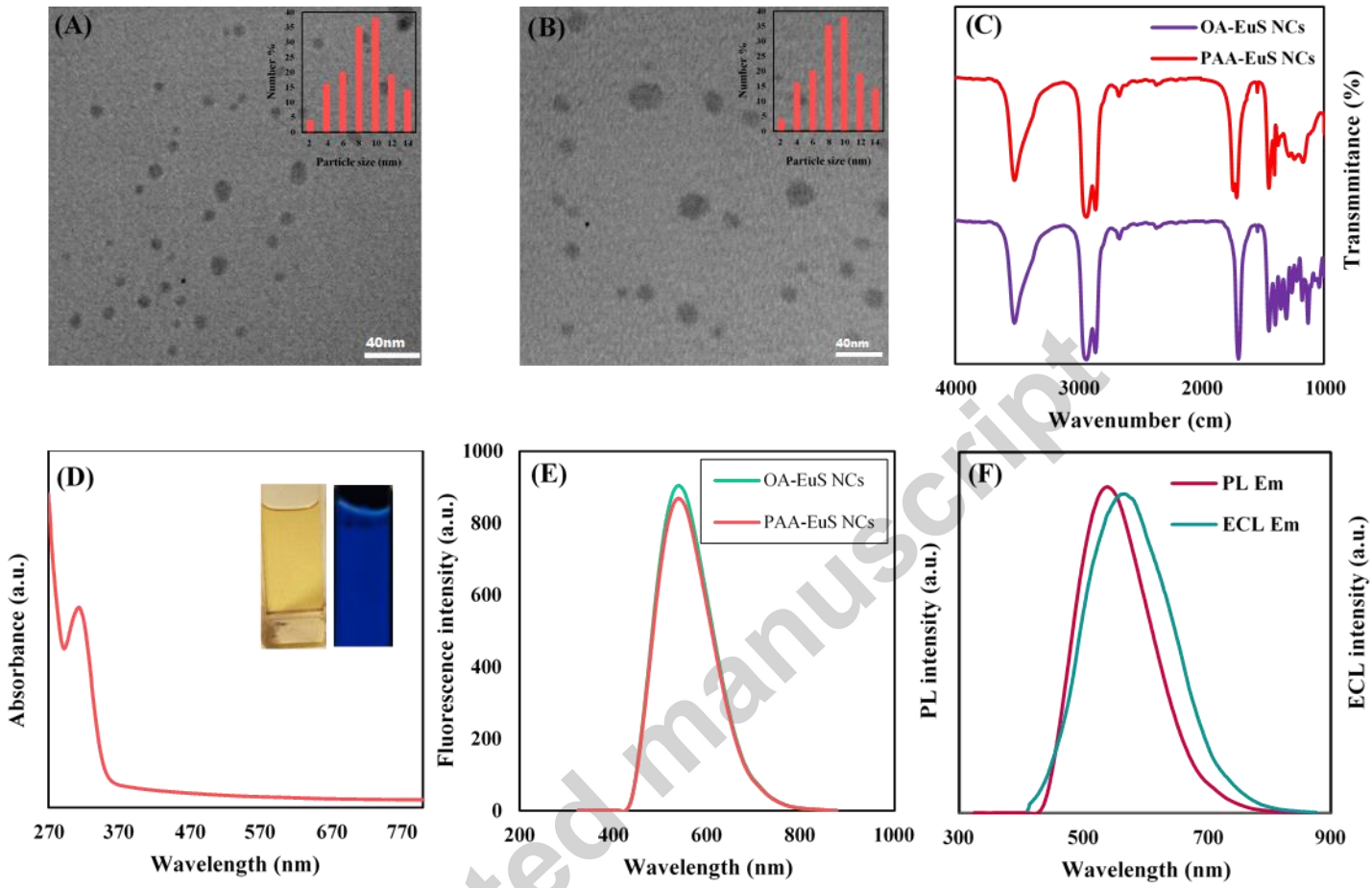

Fig.1

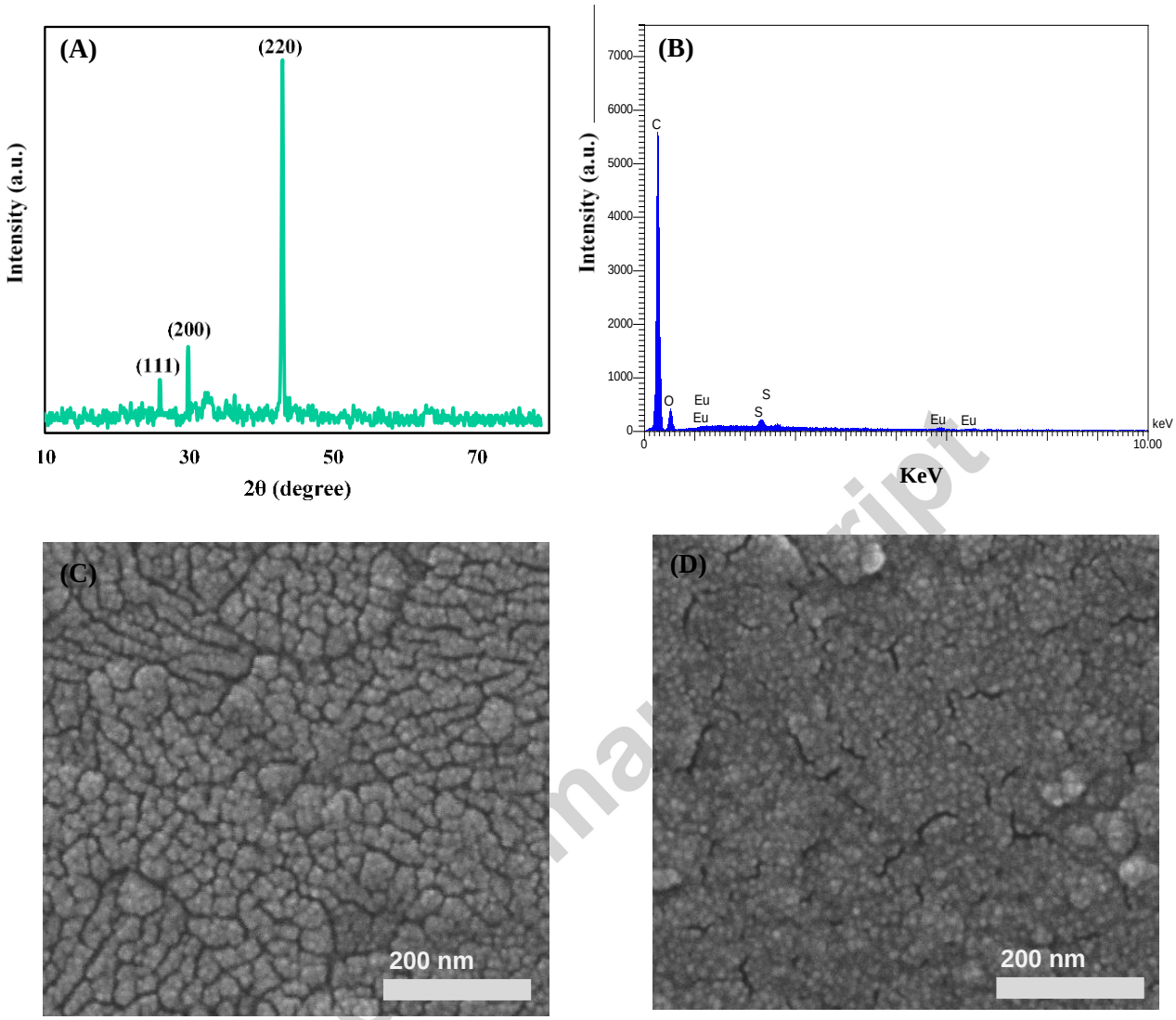

Fig.2

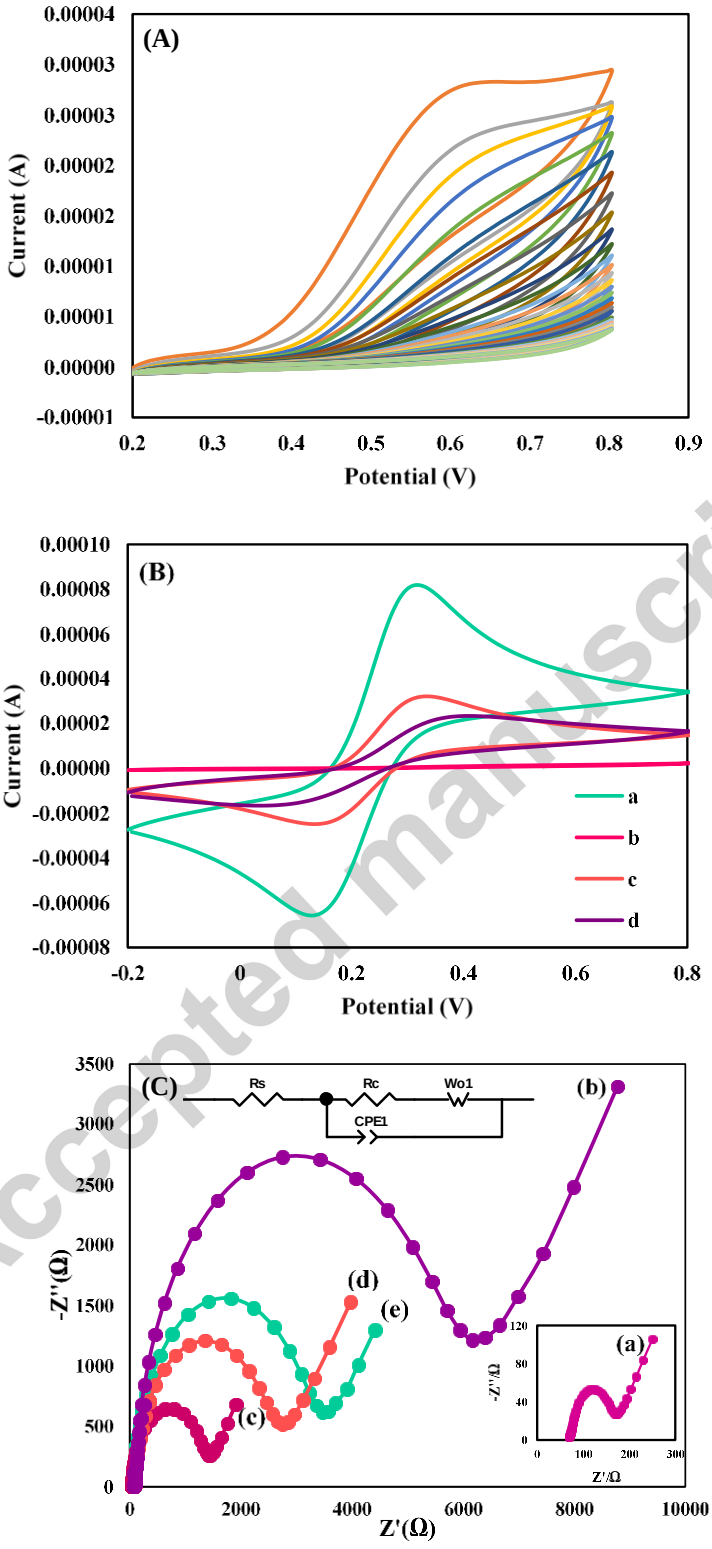

Fig.3

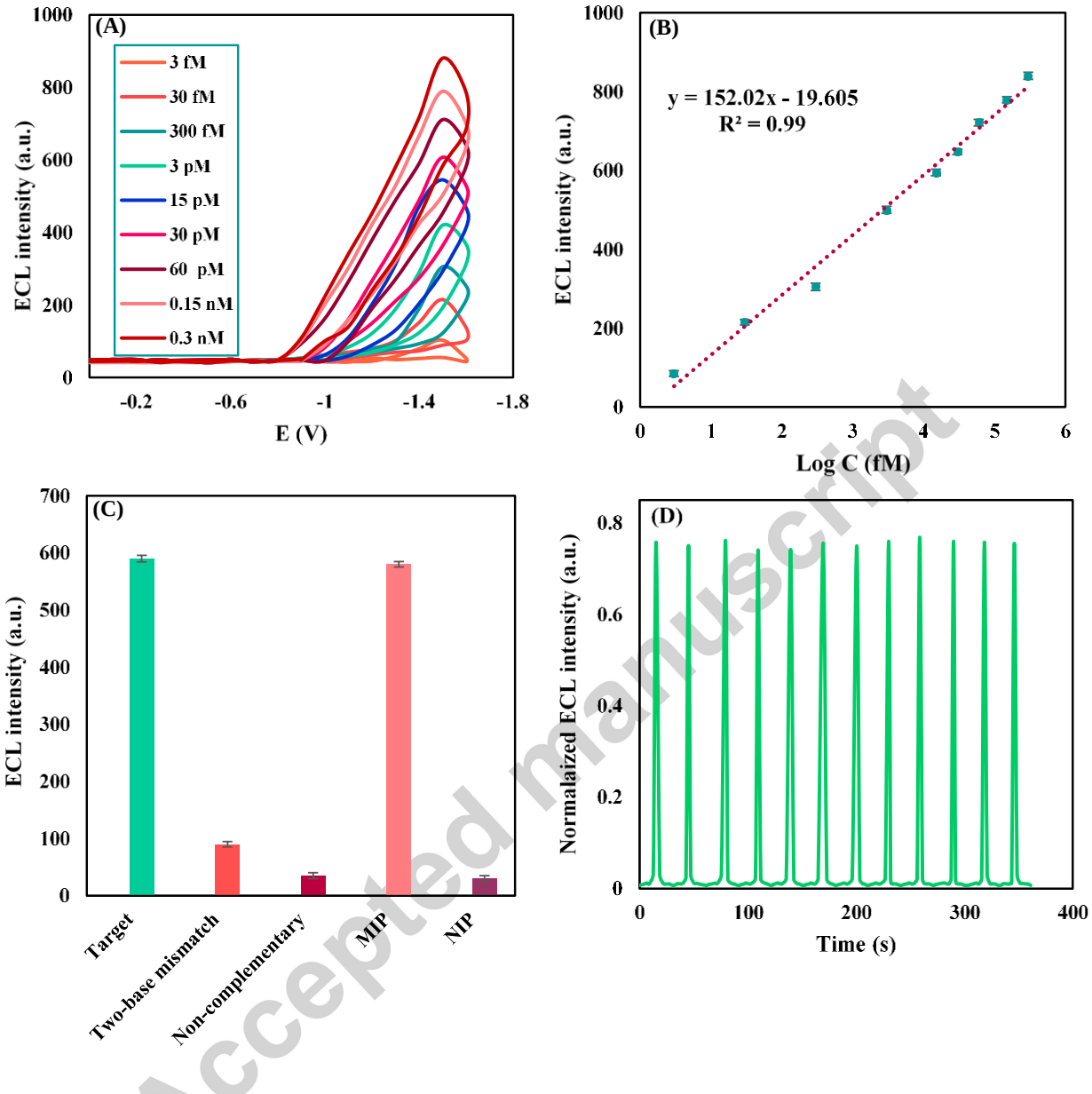

Fig.4

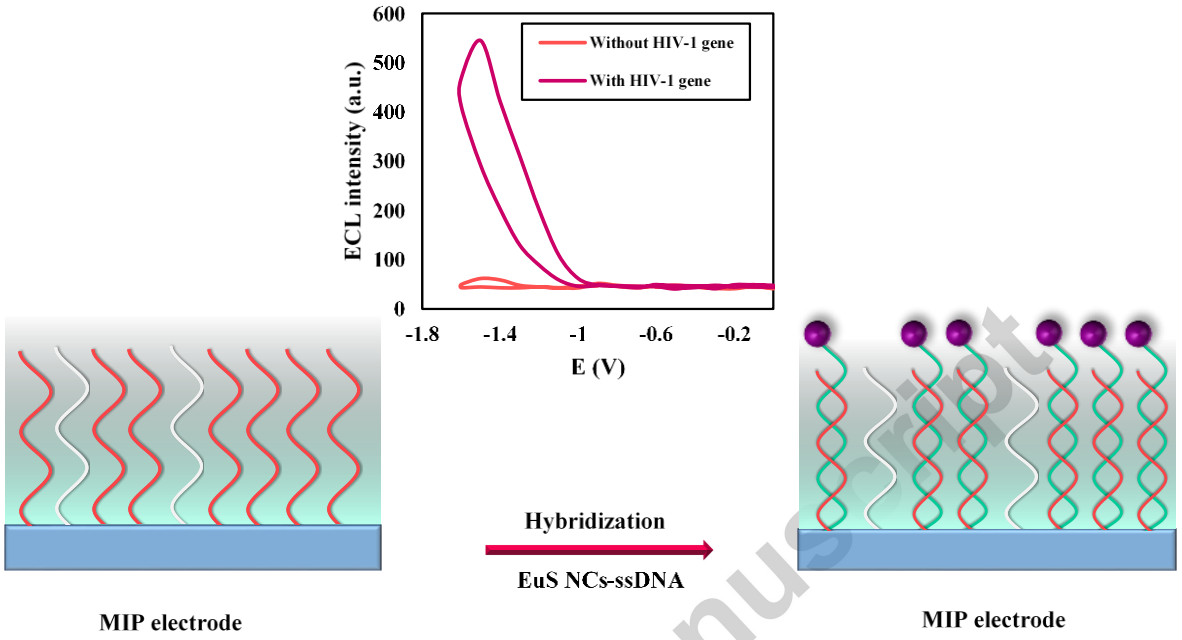

Graphical Abstract

Highlights for review

Sensitive MIP electrochemiluminescence sensor was developed for HIV-1 gene detection.

EuS nanocrystals used as novel luminophore for development of MIP-ECL sensor.

Sensor applied for HIV-1 gene detection at range of 3.0 fM - 0.3 nM and DL was 0.3 fM.

The application of sensor for analysis of HIV-1 gene in real human serum was evaluated.